8

Experimental Heat Conductin Study of Fastener Jointed Structural Components

Kunihiko OHTAKE and Shuuji ENDO
Structural Mechanics Division
National Aerospace Laboratory
Tokyo, Japan

Nobuhiro UCHIDA
Nagoya Aerospace Systems
Mitsubishi Heavy Industry Co., Ltd.
Nagoya, Japan

Abstract

We have studied experimentally the heat conductance characteristics of an aluminium alloy, fastener jointed structure. Our study consisted of the measurement of contact thermal resistance and the temperature distribution of jointed structural components. The result shows that near the jointed edge heat conduction is disturbed because of the existence of the contact surface. This effect is remarkable when the test environment is a vacuum.

1. Introduction

The skin surface of a hypersonic transport aeroframe faces very high heat flux because of aerodynamic heating. Therefore the structural designer should consider the thermal stresses and heat conduction. The aeroframe structure is composed of many components, which are the assembleges of the fastener jointed thin structural members. So, for aeroframe heat conduction analysis, we suppose that the effects of contact thermal resistance between the contact surfaces should be considered.

Our experimental heat conduction study of jointed structures is devided into three phases. The first is the measurement of contact thermal resistance of two kinds of aluminium alloies, 2024-T62 and 7075-T6, which are frequently used in aeroframes. The second is the estimation of contact thermal resistance of a fastener jointed 2024 aluminuum plate component[3]. The third is the temperature responce measurement of a fastener jointed structural component with a branch. The last one is intended for example data for the numerical simulation model of jointed plate structures. In this case several heat conduction factors affect the measured temperature distribution in realistic simulation. In particular, convection effects seem very complex, and we excute our measurements both in a vacuum and in an atmospheric environment in order to treat the convection effect separately in the analysis.

2. Direct measurement of contact Thermal Resistance(Ph.1)

2.1 Test equipment and experimental method

The sketch of the test equipment is shown in Fig. 1. The test pieces are as followings;

materials: 2024-T4 and 7075-T6, anticorrosive process on the surface
geometries: diameter 30mm, thickness 2.03mm, poker chip shape

Two chips of the same material are placed face to face, and are sandwiched between stainless steel rods (sus304) of the same diameter . Each rod is equipped with six small holes for the measurement of axial direction temperature distribution. A rubber sheet electrical heater is pasted on the upper face of one rod, and a water cooled cold plate is attached to the bottom face of the other rod. Thermocouples are inserted into the rods. The side of the whole specimen is coverd by an insulater. The universal test machine gives the axial compressive loads to the contact surface of the poker chips.

Durring the test, assumed compressive pressure is loaded, the top is heater loaded, and the bottom is cooled for the specimen. After thermal balance is attained, temperature measurement is carried out for 12 point. During the test, the coolant water temperature of the cold plate is hold to 20℃. The supplied heat power is 20W for the 2024-T62 test piece, 30W for the 7075-T6 testpiece. The contact surface pressure is 0.1, 1, 10 and 50MPa. Fig. 2 shows the temperature distribution model of the specimen. The heat flux density is

$$q = -\lambda_1 \frac{dT_1}{dX} = -\lambda_2 \frac{dT_2}{dX} \qquad (1)$$

where $\lambda 1$ is thermal conductivity of the test piece, $\lambda 2$ is that of the stainless rod. The thickness of the poker chip test pierce is dX , so the difference of the upper rod contact surface temperature T21(2) and the lower rod contace surface temperature T12(2) is given by

$$T_{12(2)} - T_{21(2)} = -\{\Delta T_{21} - 2\frac{dT_1}{dX}\Delta X + \Delta T_{11} + \Delta T_{12}\} \qquad (2)$$

where suffix(2) denotes that two chips are used and:

dT21 : temperature drop between rod and test pierce contactsurfaces
dt11 : temperature drop between two test pierce contact surfaces.
dt12 : temperature drop between test pierce and rod surfaces

The experimental temperature measurement gives the temperature gradient in the rod. T12(2) and T21(2) are obtained from the extrapolation of the measurement.

After that , one poker chip test pierce is removed , and similar measuement is carried. In this case The difference of the upper contact surface temperature T21(1) and the lower contact surface temperature T12(1) is given by

$$T_{12(1)} - T_{21(1)} = -\{\Delta T_{21} - \frac{dT_1}{dX}\Delta X + \Delta T_{12}\} \qquad (3)$$

The contact surface temperatures T21(1) and T12(1) are also obtained by extrapolation. Here it is obvious that dT11 can be extruded from the easy operation using eqns. (2) and (3). Therefore we can get the value of the test pierce contact thermal resistance Rh11. as

$$R_{h11} = \frac{\Delta T_{11}}{q} \qquad (4)$$

If we assume that dT21=dT12, then we can get Rh21= Rh12. Precisely, it is observed that the contact thermal resistance from aluminium alloy to steel is less than the resistance from steel to aluminium alloy[1].

We use the following thermal conductivity values for the calculation[2].

matelial	thermal conductivity (W / m・K)
2024-T62	120
7075-T6	130

SUS 304 16

2.2 Experimental Results

Fig. 3 shows the relation between contact pressure and contact thermal resistance. The experiment assumes one-dimensional heat conduction, but the heat leak through the side insurance is not negrigible. Therefore the temperature gradient in the rod is not linear, which disturbs the precise extrapolation of temperature at the contact surface. Under such a condition, our observations are:

(1) The contact pressure increase causes the reduction of contact thermal resistance. This is reasonable because of the fact that the pressure increase generates a larger direct contact area.

(2) The difference of contact thermal resistance between the two materials, 2024-T62 and 7075-T6, is not large in this experiment. This result is caused by the small defference of the two materials' hardness and thermal conductivity.

(3) If the contact pressure is more than 10MPa, then contact thermal resistance between aluminium surfaces, Rh11, becomes a constant value. But contact thermal resistance between stainless steel and aluminium alloy, Rh21, is still decreasing. This is considered to be due to the difference of the two materials' hardness and surface roughness.

3. Heat conduction test of lap jointed member.(Ph.2)

3.1 Test specimen and experimental method.

The specimen is a lap joint type. Two pierces of aliuminium alloy plate is fastened by 4 bolts. The diameter of the bolt is 4.8mm. The plate is made from 2024-T62 and the thickness is 2.03mm. A rubber type electric heater is pasted at the top surfaces of the plate. A cold plate is attached at the lower angled part. The total specimen is shown in Fig. 4.

In the experiment the bolt is fastened to the defined torque. Then the specimen is set in a vacuum chamber. The heater supplies thermal loads and the cold plate takes the role of the fixed temperature boundary. After the system is thermally balanced, temperature is measured by the thermocouples which are welded on the plate surfaces. Vacuum (less than 0.5 torr) and atmosphire environments are used for the test. The electric power of the heater is 60W. The coolant water temperarute is holded to 20℃ during the test. The fastening torqu is changed to 20, 40, and 60 kgf. cm.

3.2 Experimental Results

Fig. 5 shows the temperature plot along the heat flow direction distance. In all 6 cases, a temperature gap is observed at the lap joint part. Fig. 6 is a heat conduction model for the specimen. Fig. 6(a) is based on the assumption that the jointed part consists of one continuum body. The temperature gradient of the joined part is assumed to be one half of the gradient of the regular part, an anti-proportional assumption to the sectional area. Fig. 6(b) shows a contact model for the lapped contact surface. Here the assumption for the temperature gradient of the lapped part is the same as for the continuum model. In addition, exsistence of a temperature drop dT due to the contact thermal resistance is assumed on the contact surface. Denoting the temperature of each contact surface as T1 and T2, and the overlapping part length as L, the temperature difference of this part is expressed as

$$T_2 - T_1 = -\left\{\Delta T - \frac{1}{2}\frac{dT_1}{dX}L\right\} \qquad (5)$$

T1, T2 and the temperature gradient of (5) is obtained from the experimental measurement.
where :

T21(2) : upper rod contact surface temperature

T12(2) : lower rod contact surface temperature

THerefore dT can be calculated. In addition, heat flux q2 through the contact srface is written as

$$q_2 = \frac{t}{L}(-\lambda)\frac{dT_1}{dX} \qquad (6)$$

where t is the single plate thickness.
Then, using this dT and q2, the contact thermal resistance extruded from this test shoud b e;

$$R_H = \frac{\Delta T}{q_2} \qquad (7)$$

Fig. 7 shows the relation between the fastening torque and contact thermal resistence Rh. In addition the upper horizontal scale stands for the contact pessure, which is calculated from the relation between fastening torque and force. From this graph, the following results are derived.

(1) The value of contact thermal resistance is larger in a vacuum than at atmospheric pressure. If the mean free path of the filler gas in the contact surface gap is less than the gap dimension, which is caused by the chamber pressure reduction, then the contribution of filler gas to the heat conduction between two surfaces should be reduced[4].

(2) The differences of resistance values among the different torques are not so distinguishable. This comes from the large fastening torque engaged in the test. Then the contact surface conditions become thermally equivalent. But precise observation detects that the increase in torque causes a small increase in resistance, which contradicts the results of the preceeding section. This is explaind by the fact that the large fastening torque causes a delicate deformation of the plate part away from the bolt, which causes insufficient contact in the area. In addition, the fastening torque of an aeroframe high rock bolt of this size is about 35 to 46 kgf. cm. Therefore the setting level of torque is reasonable for aeroframe application.

(3) The contact thermal resistance calculated in this section is about 10 times larger than that of the preceeding section. For comparison, of course, the torque is changeg to the equivalent contact pressure. The one dimensional heat conduction model assumption of Fig. 6 seems insufficient for this lap joint case. The estimated value, Rh of eqn. (7) should be called "system resistance value", which should be regarded as a different concept from the direct measured value.

4. Heat conduction test for the fastener jointed component with branch member.(Ph.3)

4.1 Test piece, test equipment and experimental method.

Five test pierces are classified into two series which are described in Table 1. The features of the test pieces are shown in Fig. 9. In the T series, an angle member is jointed to a plate with a fastener. The material is 2024-T62 anticorrosively processed aluminium alloy. The widths of the lapped parts are 30mm and 50mm. The number of fasntener bolts are 6 x 1 and 6 x 2, where the second number stands for the column. The distance between the bolts is 25mm. The fastening torque is 46 kgf. cm. In the r series, two folded plates with a radius of 10mm are fastener jointed. The lapped part width are 12mm, 20mm and 30mm. The torque is 45 kgf. cm for r1 and r2, and 40 kgf. cm for r3. The number of fasteners is 4 x 1

for r1 and r2, 4 x 2 for r3. The fastener distance is 30mm for r1 and r2, 50mm for r3. For all cases standard aeroframe fasteners are engaged. Rubber heaters of 50 mm x 150mm are pasted on the top face of each piece . The one heater electric capacity is 60W. We refer to the heater sides as "top" or "upper" and the opposite side as "bottom" or "lower" afterwards. At the bottom branched end, cooling tubes made of copper are connected with screws. Thermocouples are spot welded on the center line of the specimen.

The test equipment system is shown in Fig. 10. The specimen is set inside the vacuum chamber. The transformed electric power is supplied to the rubber heater through the vacuum connecter. The constant temperature water reserver supplies coolant water to the copper tube. The temperature is measured by the data logger of 60 points per second scanning speed which is operated automatically by the personal computer. The pressure condition of the chamber is the same as in the preceeding section, ie, vacuum or atmosphere.

4.2 Test results

Thirty minites after the power is turned on, thermal equiliblium is obtained, and temperature measurement is carried out. The results are shown in Fig. 10.

(1) In the lapped part, at least within 10mm from the upper lapped edge, the surface temperature of the heated plate, which is called the main plate, is higher than the opposite surface temperature of the branched plate.

(2) The temperature difference of (1) is remarkable in a vacuum but very small in atmospheric condition.

(3) The temperature difference is small in the off lapped, lower part.

(4) For the T series specimen, at the lapped lower edge region , the temperature of the branched plate is higher than that of the main plate.

(1) and (2) is the effect of the contact thermal resistance. This is also verified by an addditional test, where continuum and fastner joined step shaped plates are compared for the temperature measurement. The reason for (4) has not yet been well analised. There are several facts to be noted: 1) the branched plate is a little bit thin by about 0.05mm, 2) the inside of the angle corner is very thick, 3) distance definition is different between flat plate and corner.

5. Concluding comment

We studied, under relatively low heat flux, the heat conduction characteristics of the structural components which have lapped and fastener jointed part. The fastener jointed aeroframe is thermally very strongly connected under atmospheric conditions. We are much interested in the very weakly contacted part and /or very strong heat flux condition.

References

1) Y. Katto: Dennetsu Gairon, Youkenndo, 1964
2) JSME: Heat transfer handbook 4th ed. 1986
3) NAL J-94004, pp. 125-132, 1994
4) JSAAE/JSME pp. 357-361, 1994

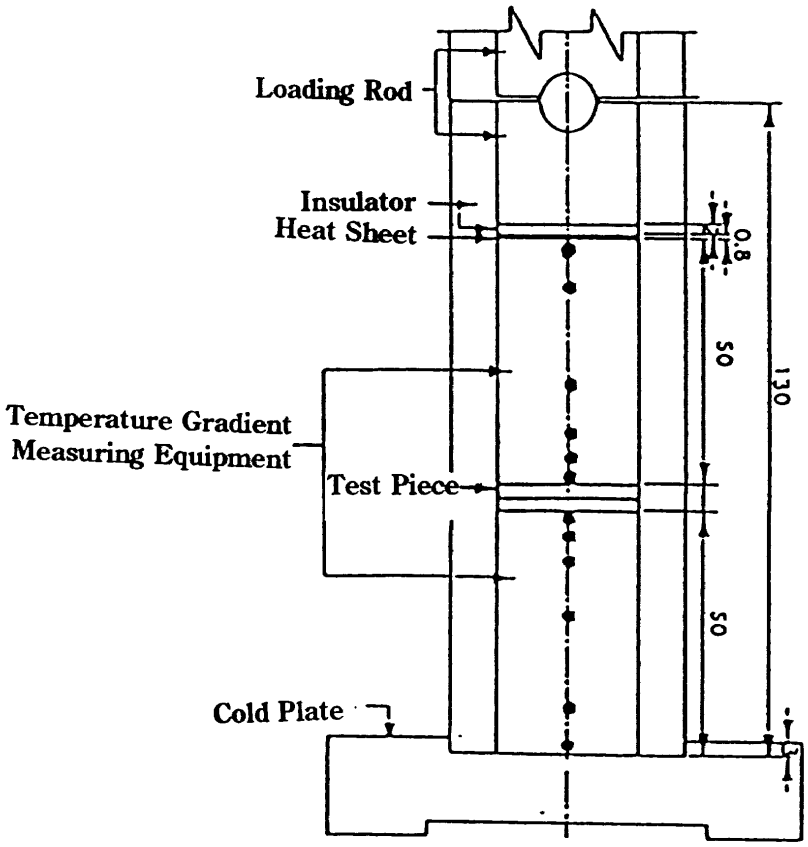

Fig.1 Test Equipment for Ph.1 Test

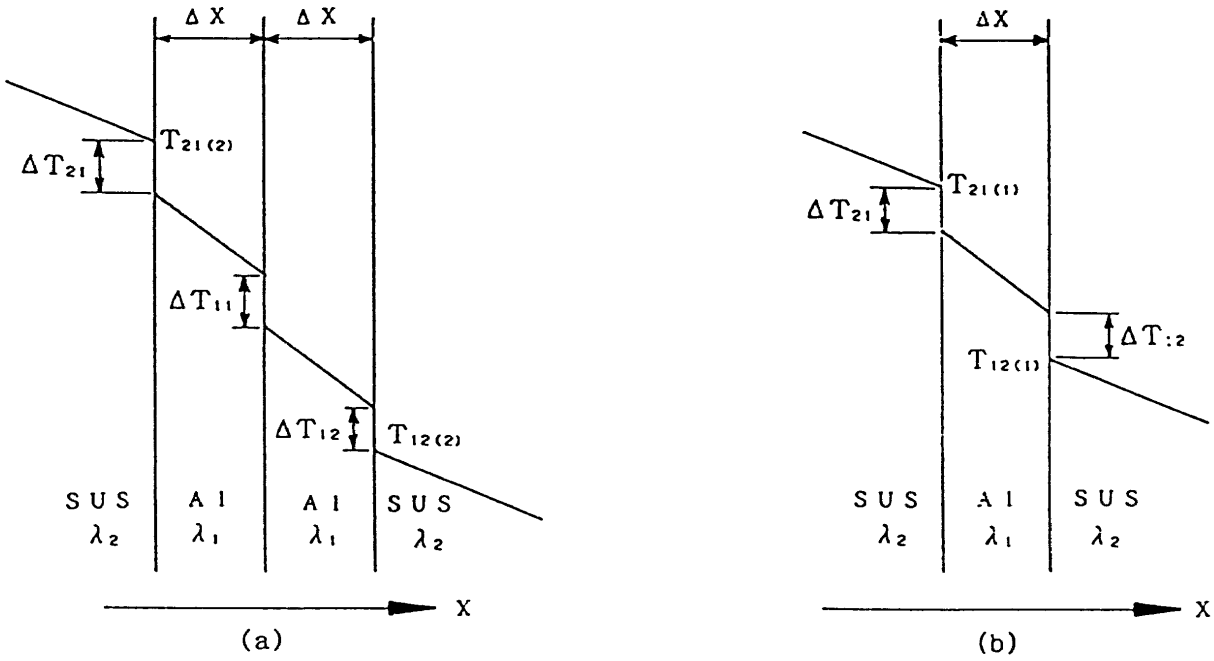

Fig.2 Temperature Distribution Model for Ph.1 Test

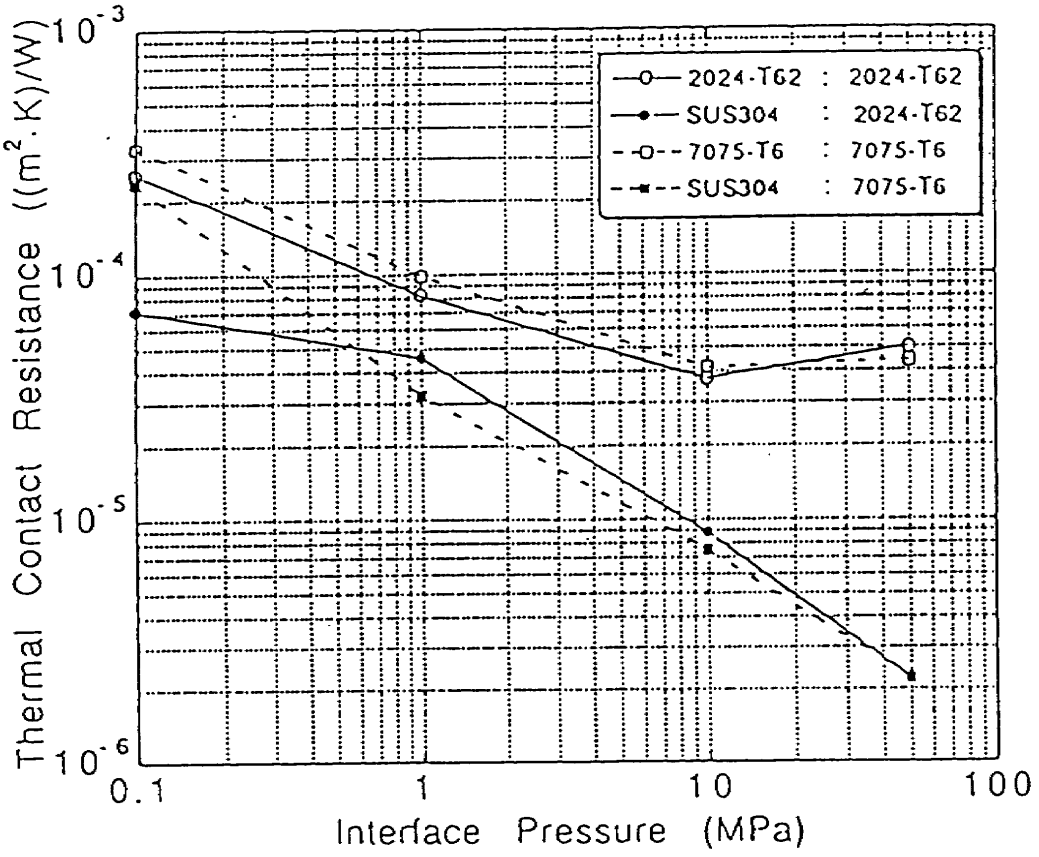

Fig.3 Relation between Contact Pressure and Contact Thermal Resistance

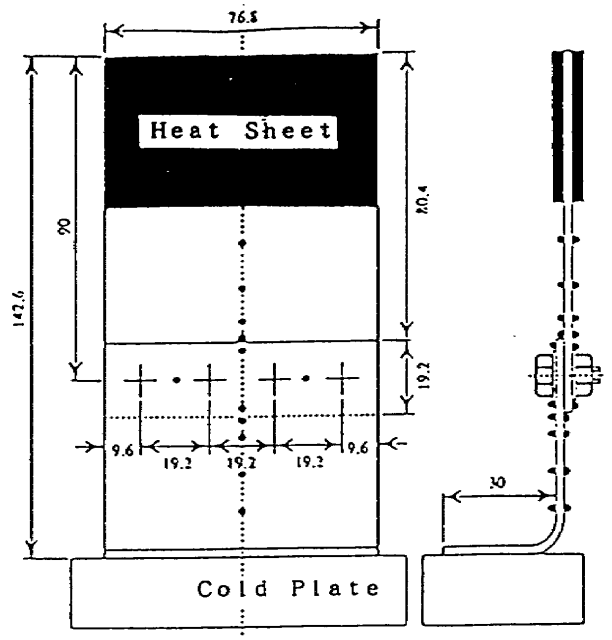

Fig.4 Test Equipment for Ph.2 Test

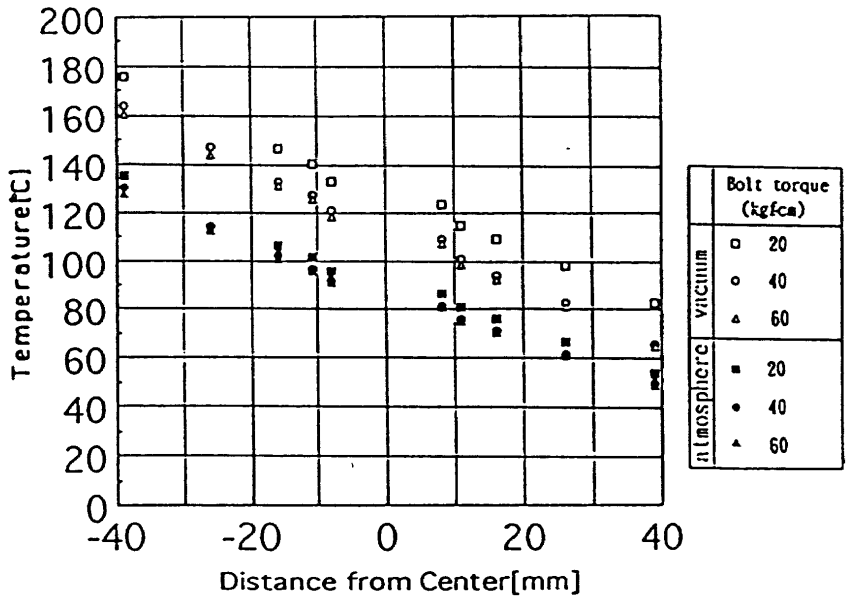

Fig.5 Temperature Distribution along the Heat Flow Direction

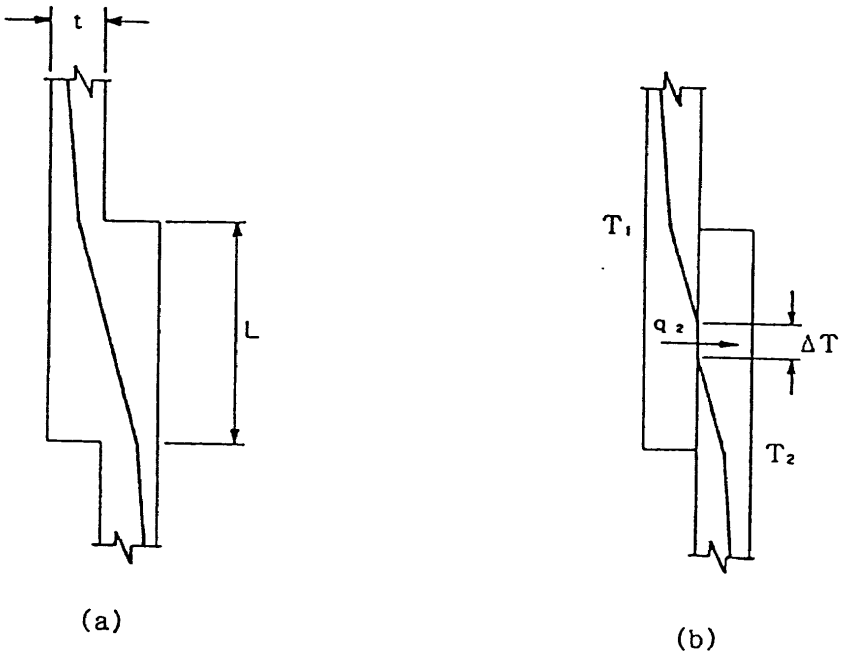

Fig.6 Temperature Distribution Model For Ph.2 Test

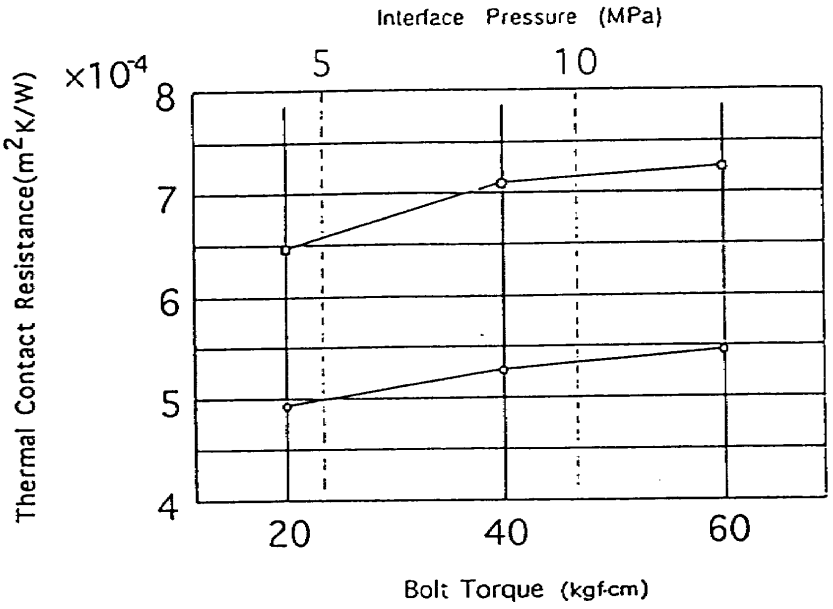

Fig.7 Relation between the Fastening Torque (or Contact Pressure) and Contact Thermal Resistance

Table 1 Test Piece Geometrics for Ph.3 Test

test piece type	width mm	lapped length mm	number of fastener	fastening torque	fastener pitch mm
T 1	150	30	6 x 1	40lb.inch	25
T 2	150	50	6 x 2	40lb.inch	25
r 1	150	12	4 x 1	45kgf.cm	30
r 2	150	20	4 x 1	45kgf.cm	30
r 3	150	40	4 x 2	45kgf.cm	50

material:2024, thickness:2mm, heater:50x150mm 60Wx2, coolant:2l/min.

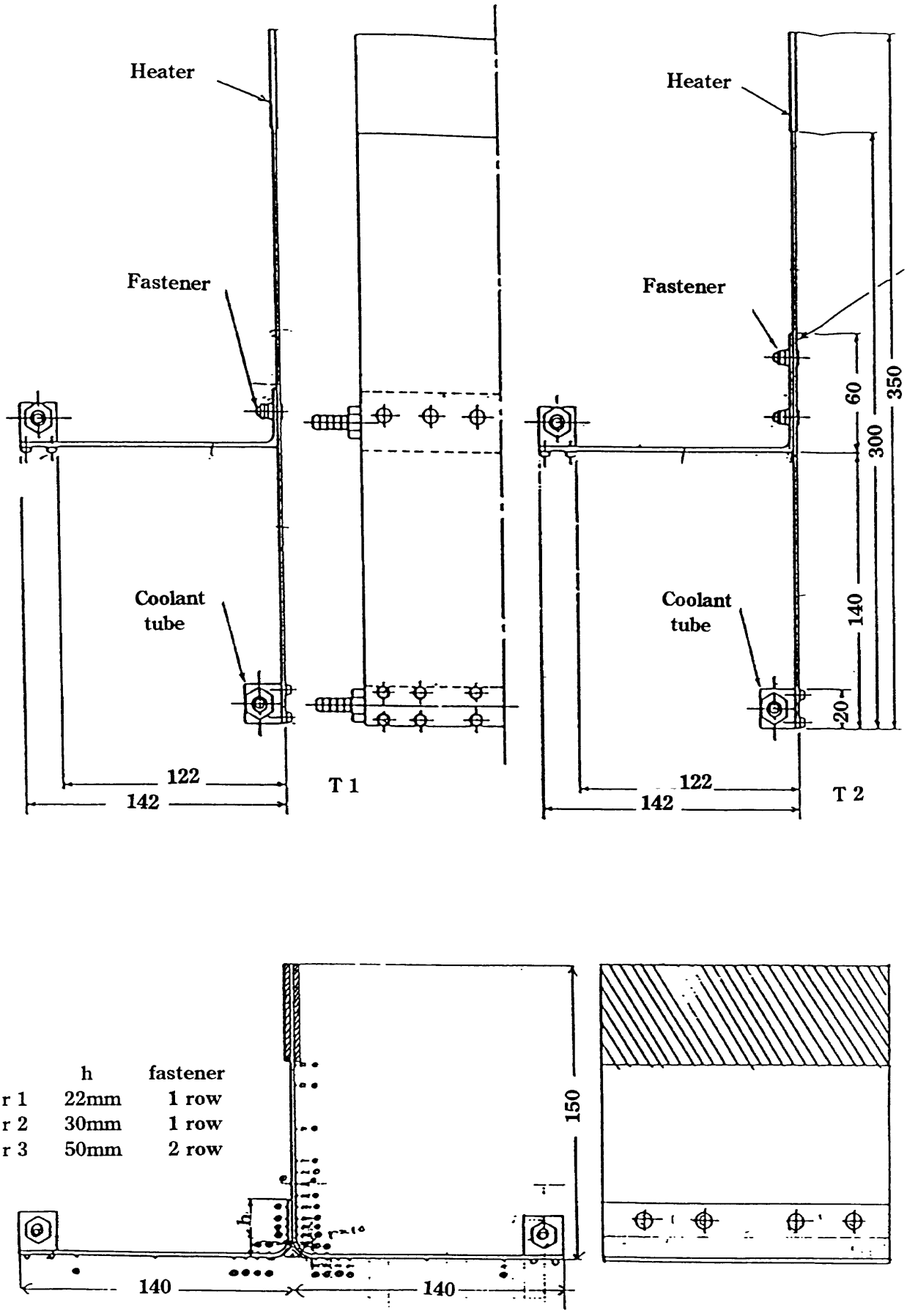

Fig.8 Test pieces for Ph.3 Test

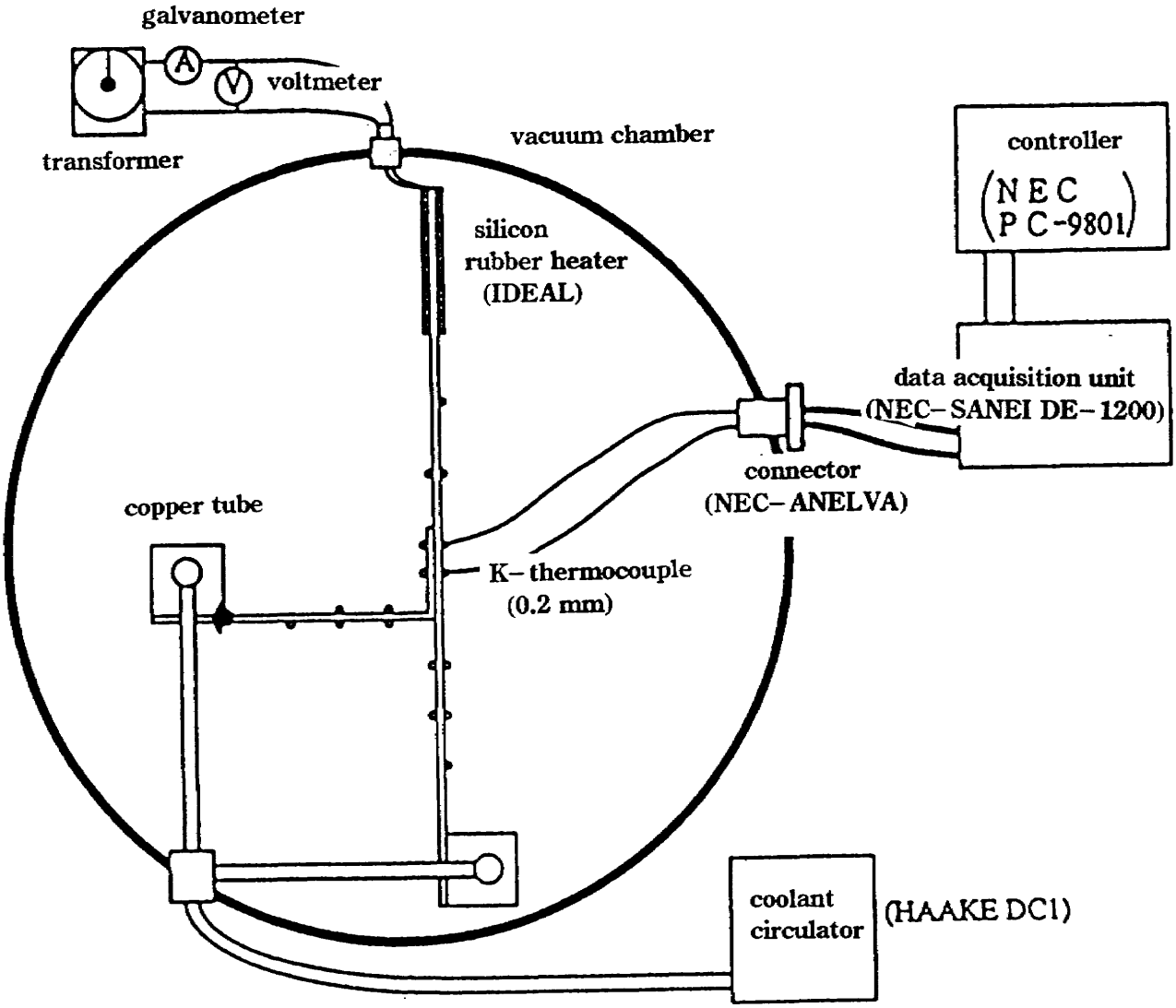

Fig.9 Test equipment for Ph.3 Test

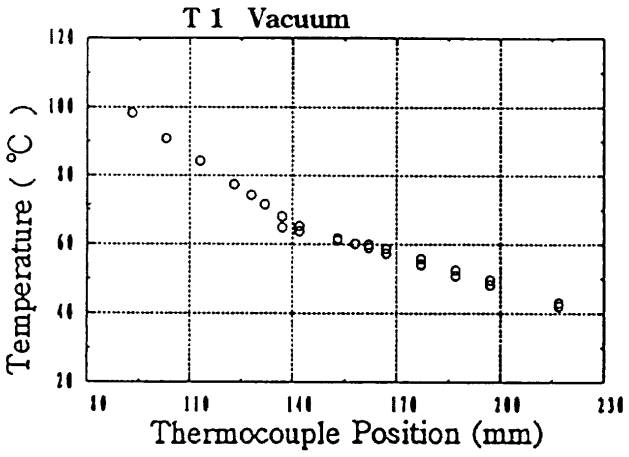

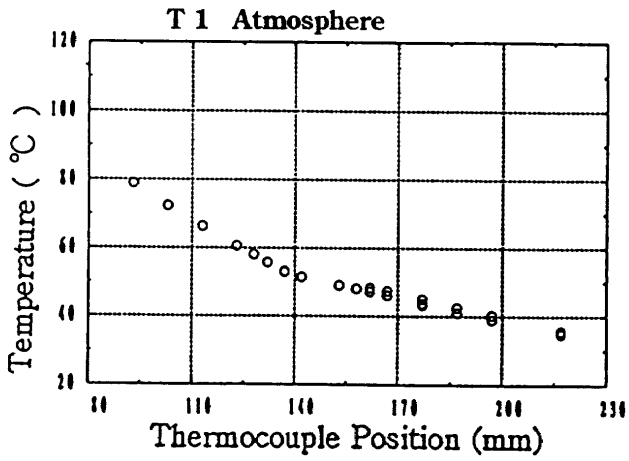

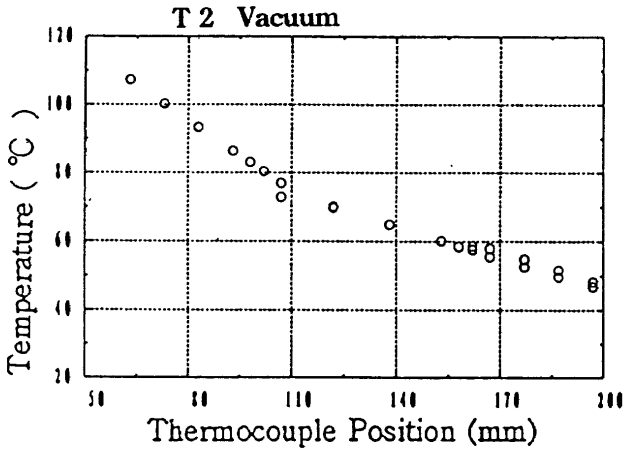

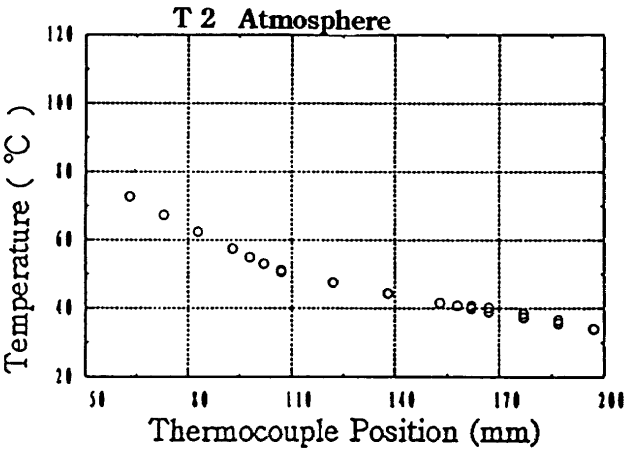

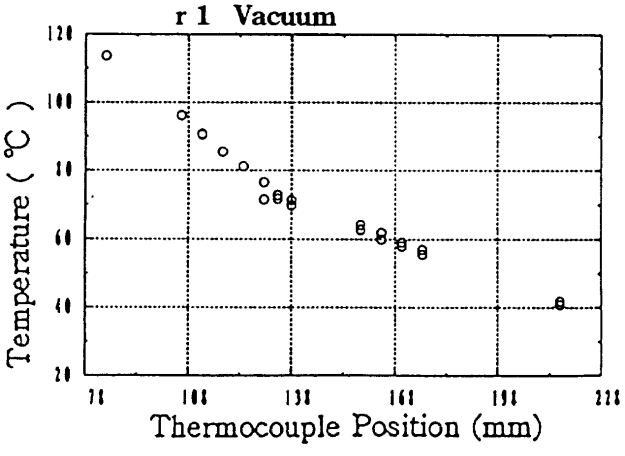

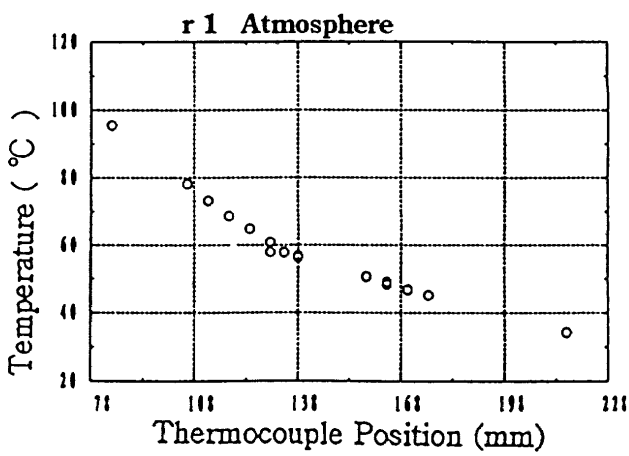

Fig.10−1 Temperature Distribution along the center line at 30 min. after the heat start for Ph.3 Test

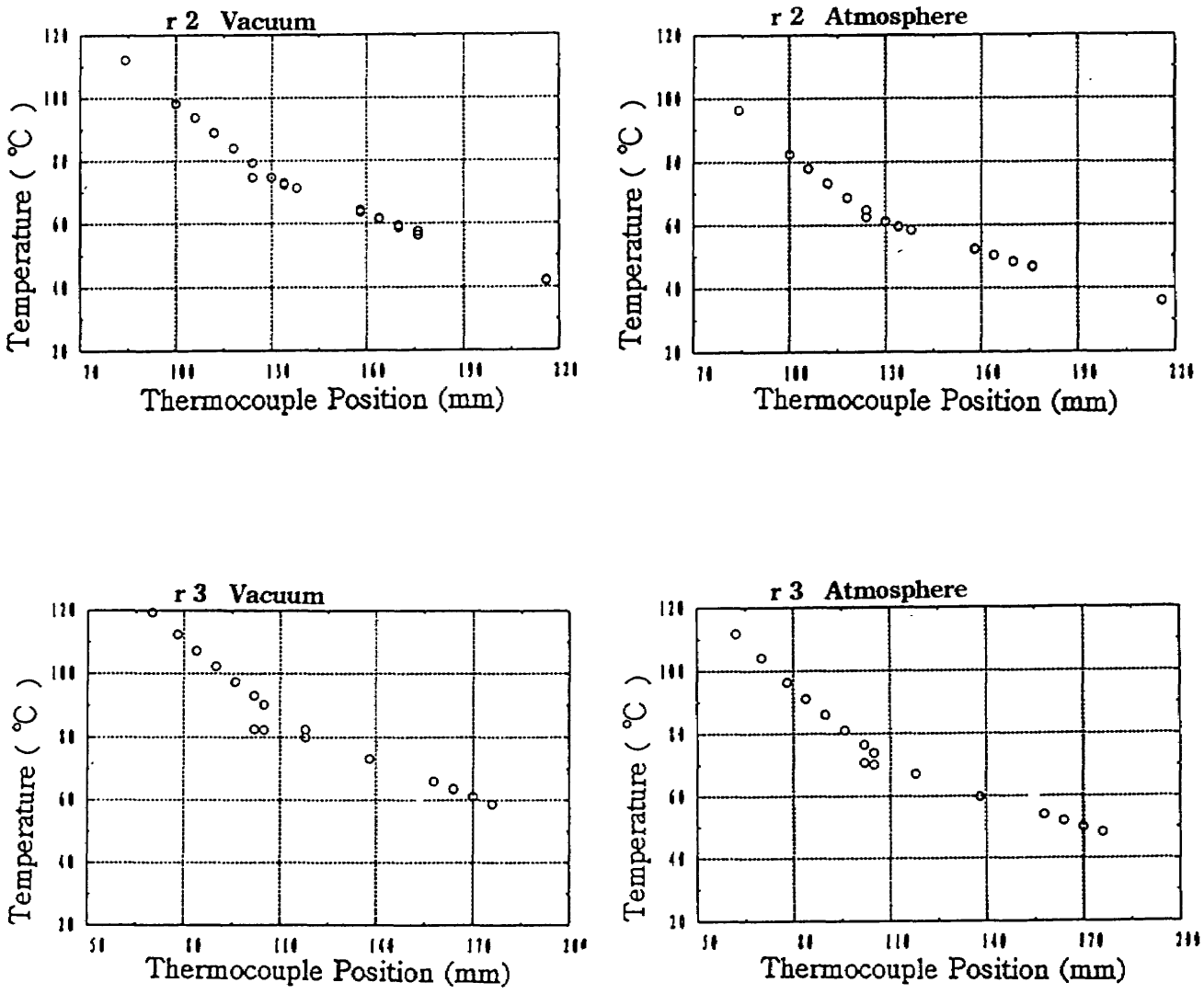

Fig.10–2 Temperature Distribution along the center line at 30 min. after the heat start for Ph.3 Test